mental parameters. Nevertheless, the qualitative trends in a wide variety of experiments give a clear indication of the importance of phase fluctuations in high-temperature superconductors. □

Received 28 October 1994; accepted 6 March 1995.

1. Schrieffer, J. R. *Theory of Superconductivity* (Benjamin, New York, 1964).
2. Anderson, P. W. in *Quantum Fluids* (ed. Brewer, D. F.) 146–171 (North-Holland, Amsterdam, 1966).
3. Emery, V. J. & Kivelson, S. A. *Phys. Rev. Lett.* (in the press).
4. Adler, J., Holm, C. & Janke, W. *Physica* A**201,** 581–592 (1993).
5. Olsson, P. & Minnhagen, P. *Physica Scripta* **43,** 203–209 (1991).
6. Batlogg, B. in *High Temperature Superconductivity* (eds Bedell, K. S., Coffey, D., Meltzer, D. E., Pines, D. & Schrieffer, J. R.) 37–82 (Addison-Wesley, Redwood City, 1990).
7. Mehring, M. *Appl. magn. Reson.* **3,** 383–421 (1992).
8. Basov, D. N., Timusk, T., Dabrowski, B. & Jorgensen, J. D. *Phys. Rev.* B**50,** 3511–3514 (1994).
9. Wachter, P., Bucher, B. & Pittini, R. *Phys. Rev.* B**49,** 13164–13171 (1994).
10. Emery, V. J. & Kivelson, S. A. *Physica* C**209,** 597–621 (1993).
11. Uemura, Y. J. *et al. Phys. Rev. Lett.* **62,** 2317–2320 (1989).
12. Uemura, Y. J. *et al. Phys. Rev. Lett.* **66,** 2665–2668 (1991).
13. Schneider, T. & Keller, H. *Phys. Rev. Lett.* **69,** 3374–3377 (1992).
14. Pokrovskii, V. L. *Pis'ma Zh. Teor. Fiz.* **47,** 539–541 (1988); English translation *JETP Lett.* **47,** 629–632 (1988).
15. Cautadella, V. & Minnhagen, P. *Physica* C**166,** 442–450 (1990).
16. Randeria, M., Trivedi, N., Moreo, A. & Scalettar, R. T. *Phys. Rev. Lett.* **69,** 2001–2004 (1992).
17. Lynton, E. A. *Superconductivity* (Methuen, London, 1962).
18. Orlando, T. P., McNiff, E. J. Jr, Foner, S. & Beasley, M. R. *Phys. Rev.* B**19,** 4545–4561 (1979).
19. Maple, M. B. *et al. Phys. Rev. Lett.* **54,** 477–480 (1985).
20. Gross, F., Andres, K. & Chandrasekhar, S. *Physica* C**162–164,** 419–420 (1989).
21. Fischer, O. *Appl. Phys.* **16,** 1–28 (1978).
22. Uemura, Y. J. *et al. Nature* **352,** 605–607 (1991).
23. Ramirez, A. P. *Superconductivity Rev.* **1,** 1–101 (1994).
24. Uemura, Y. J. *et al.* in *Organic Superconductivity* (eds Kresin, V. Z. & Little, W. A.) 23–29 (Plenum, New York, 1990).
25. Wu, D. H. *et al. Phys. Rev. Lett.* **70,** 85–88 (1993).
26. Uemura, Y. J. *et al. Nature* **364,** 605–607 (1993).
27. Niedermayer, Ch. *et al. Phys. Rev. Lett.* **71,** 1764–1767 (1993).
28. Weber, M. *et al. Hyp. Int.* **63,** 93–102 (1990).
29. Weber, M. *et al. Phys. Rev.* B**48,** 13022–13036 (1990).
30. Franck, J. P., Harker, S. & Brewer, J. H. *Phys. Rev. Lett.* **71,** 283–286 (1993).
31. Basov, D. N. *et al. Phys. Rev. Lett.* **74,** 598–601 (1995).

ACKNOWLEDGEMENTS. This work was supported by the US NSF and the Division of Materials Science, US Department of Energy.

Electric-field-induced pattern formation in colloidal dispersions

M. Trau, S. Sankaran, D. A. Saville & I. A. Aksay

Department of Chemical Engineering and
Princeton Materials Institute, Princeton University, Princeton,
New Jersey 08544–5263, USA

THE formation of patterned colloidal structures from dispersions of particles has many potential uses in materials processing[1–3]. Structures such as chains of particles that form in the presence of electric or magnetic fields are also central to the behaviour of electrorheological fluids[4–6] and ferrofluids[7]. Electrohydrodynamic effects in aqueous suspensions have been described by Rhodes *et al.*[8]. Here we show that such effects can be used to create structures within a non-aqueous colloidal dispersion of dielectric particles. When the conductivity of a particle-rich spherical region (bolus) is higher than that of the surrounding fluid, an electric field deforms the bolus into a prolate ellipsoid. If the conductivities are reversed (by adding salt to the surrounding fluid, for example), a disk-like shape results. In this way, we form colloidal columns, disks and more complex structures. Once formed, these could be frozen in place by solidifying the fluid matrix by gelation or polymerization[9].

We work with a simple model system—a spherical bolus containing suspended particles (region 1)—nested inside clear ambient fluid (region 2). The transition between the suspension and the clear fluid is gradual and smooth, without an interfacial tension. Its thickness is determined by a combination of brownian diffusion and sedimentation. Because of the particles, the dielectric constant, ε_1, and conductivity, σ_1, of region 1 differ from those of region 2 (that is, $\varepsilon_1 \neq \varepsilon_2$, $\sigma_1 \neq \sigma_2$). The mismatch between the dielectric constants of the two regions results from intrinsic differences between particles and fluid and polarization of any diffuse double layer (ion cloud) around each charged particle. Differences in conductivity arise from several factors: (1) particles impede ion flow and hence reduce the conductivity; (2) dissolved ions from the particles increase the local conductivity; and (3) σ_1 and σ_2 may be artifically increased by selectively dissolving a soluble salt. Left on its own and given time to come to equilibrium, the system will either become completely mixed via brownian diffusion or form a flat layer of particles owing to sedimentation. When subject to an electric field, the transition layer between regions 1 and 2 (that is, the region where ε and σ vary spatially) experiences an anisotropic electrostatic body force. This sets the suspension in motion and distorts the shape of the bolus. If mismatches in conductivity and dielectric constant are large enough, the electrohydrodynamic force will be dominant. It is this force which we exploit to manipulate the structure of a colloidal dispersion. The effect under study is not an 'electrorheological effect', although it may be present in electrorheological systems. The commonly accepted origin of the electrorheological effect is dipole–dipole interactions between the suspended particles induced by the applied field[4–6], whereas the effects under study result from bulk fluid motion induced by electrical body forces acting on the suspension.

We used 100-nm barium titanate ($BaTiO_3$) particles prepared by a hydrothermal process[10] and dispersed in castor oil. Barium titanate was chosen because it has an extremely high dielectric constant[11], typically between 300 and 10,000, depending on the crystalline form, and is a technologically useful material in both the electronic and optical component industries[12,13]. Castor oil was chosen as the fluid medium because: (1) it has a low conductivity ($\sigma = 1.8 \times 10^{-11}$ S m^{-1}); (2) fatty-acid-based oils are good dispersing media for $BaTiO_3$ particles[14]; and (3) its conductivity may easily be varied over a wide range by doping with small amounts of soluble organic salts (for example, tetrabutylammonium tetraphenylborate, TBATPB). Two experiments were performed to illustrate the importance of the conductivity mismatch in setting the direction of flow for the spherical geometry described above (see Fig. 1). In the first experiment, the conductivity of the dispersion was adjusted to be ~100 times higher than that of the clear fluid by dissolving a trace amount of an organic salt (to give 0.2 mM TBATPB) in the $BaTiO_3$ dispersion before injection. In the second experiment, the conductivity mismatch was reversed by dissolving the organic salt in the clear castor oil before injecting the dispersion. Figure 1 illustrates results from both experiments. In the sequence Fig. 1*a–d* (with higher conductivity on the inside), the spherical bolus deforms in the direction of the applied field and continues to stretch until it collides with the top electrode to form a near-perfect column. The column remains intact for several seconds until the disturbance generated at its top (see Fig. 1*d*) propagates down the entire length. In the sequence Fig. 1*e–h*, a dramatically different flow pattern is engendered by the field. Here the spherical bolus deforms orthogonal to the applied field, forming a disk shape which continues to expand laterally. After some time, a film forms across the bottom electrode. Steady (d.c.) fields were used to generate all of the patterns shown in Fig. 1, but the direction and speed of the motion is insensitive to field polarity. Similar flow patterns are induced by applying low-frequency a.c. fields (~100 Hz), which shows that the particle motions are not the result of electrokinetic phenomena; they can be explained in terms of an electrohydrodynamic flow.

In order to achieve useful pattern formation in these systems, however, the deliberate manipulation of colloidal structure over long periods of time is of much greater interest. For this technique to be useful for any of the applications mentioned earlier,

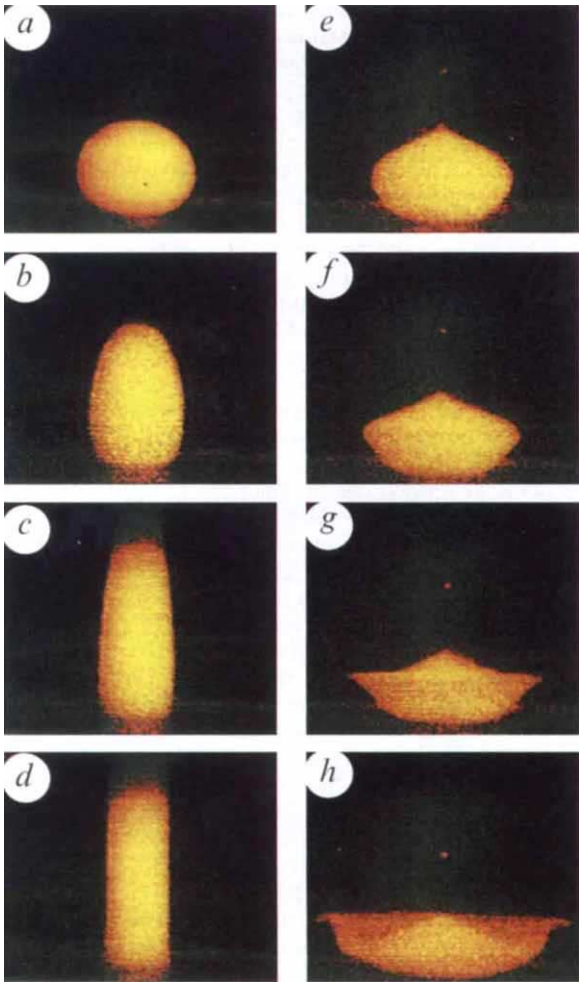

FIG. 1 *a–d* and *e–h*, Two examples of the deformation of a colloidal dispersion by means of an applied electric field. A dilute dispersion of 100-nm diameter $BaTiO_3$ particles (0.025 vol%) in castor oil was injected into clear castor oil fluid through a pinhole in a metal electrode. Slow injection of the dispersion into the clear fluid results in a spherical bolus of the dispersion nested within clear castor oil (*a*, *e*). The 4 × 4 cm metal electrodes were 1.5 cm apart; the diameter of the colloidal bolus was ~5 mm. *a–d* And *e–h* are video image sequences taken after a steady d.c. field, 2,000 V cm^{-1}, was applied in the vertical direction. The resulting photographs have been electronically coloured to enhance the contrast between particle-containing regions and clear fluid. In the two experiments the conductivity mismatch between the inner and outer bolus region was reversed by selectively dissolving a trace amount of tetrabutylammonium tetraphenylborate (TBATPB) (0.2 mM) either in the inner region (*a–d*) or in the surrounding clear fluid (*e–h*). The measured conductivity of a 0.2 mM solution of TBATPB in castor oil was 2.28×10^{-9} S m^{-1}, ~100 times higher than that of pure castor oil. The time interval between panels is ~0.2 s.

the formed colloidal structures must remain stable for a sufficiently long time to enable the surrounding fluid to be solidified by means of (for example) polymerization or gelation techniques. Unfortunately, the long-term evolution of such patterns is extremely difficult to predict for two reasons; (1) any fluid motion will deform the sample and alter the conductivity and dielectric constants from their initial values, and (2) the morphology of the transition layer (that is, both the ion- and particle-concentration profiles) will change as a result of flow induced by electrohydrodynamic, diffusion and sedimentation effects. Generally, the transition layer will become more diffuse with time. Figure 2 shows the simultaneous deformation of eight identical spherical $BaTiO_3$ suspension boli into a ringed columnar structure by the application of a steady d.c. field (500 V cm^{-1}). This type of slow deformation results in a columnar structure from each bolus. At the tip of each column a sharp spike forms, which continues to sharpen parallel to the field, stretching the column to a gradually thinner diameter (measured by laser diffraction to be <30 μm). By applying a low-frequency a.c. field (for example, 4,000 V cm^{-1}, 100 Hz in Fig. 2), colloidal spikes are formed over a much larger time period and remain stable for more than three hours before any evidence of dissipation. This time is sufficient for polymerization of the ambient fluid, as previously described[9]. Obviously, the formation of such structures is not limited to forming eight columns at a time. Multiple thin films may also be formed in this manner.

In the situations just described, motion arises from two sorts of electrical body forces, one stemming from a polarization force arising from gradations in the dielectric constant, the other due to the action of the applied field on induced free charge. Electric

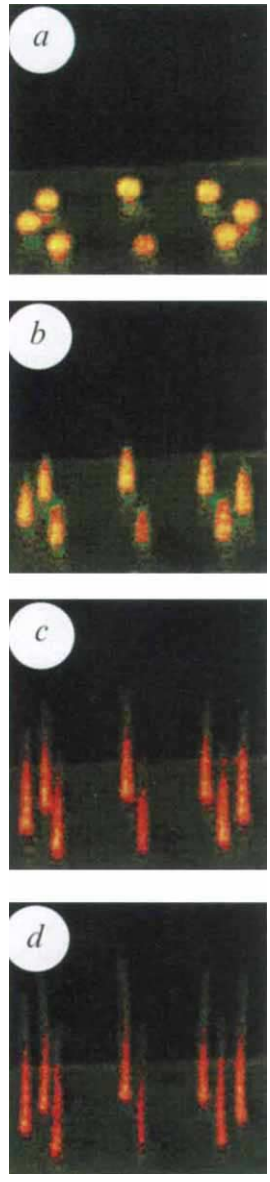

FIG. 2 The formation of multiple colloidal columns/spikes by means of electrohydrodynamic flow. *a–d* represent a sequential series of video images taken after a steady d.c. field (500 V cm^{-1}) was applied to eight identical spherical boli of the $BaTiO_3$ dispersion described in Fig. 1. The separation distance between columns is 7 mm. The slight bow in these columns is thought to be due to a hydrodynamic interaction between the columns and the vessel wall or between adjacent columns.

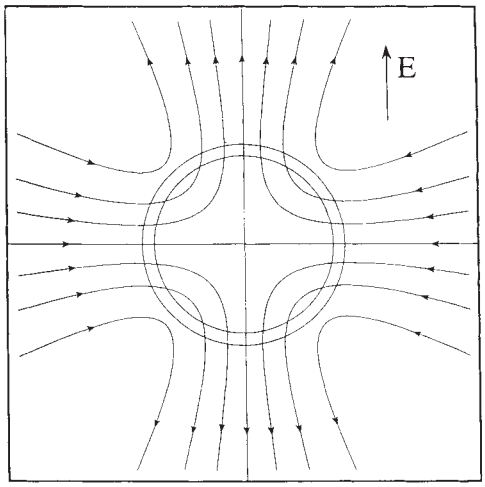

FIG. 3 Streamline pattern for flow engendered by a circular-shaped cloud of dispersion immersed in a clear fluid with a lower conductivity and dielectric constant, calculated from the model described in the text.

forces can be described in terms of Maxwell's stress tensor or as a body force[15,16], that is,

$$\mathbf{f}_e = -\tfrac{1}{2}\varepsilon_0 \mathbf{E}\cdot\mathbf{E}\nabla\varepsilon + \rho_e \mathbf{E}$$

where $\mathbf{f}_e$ is the electric body force per unit volume, ε_0 is the permittivity of free space, $\mathbf{E}$ is the electric field strength, $\nabla\varepsilon$ is the gradient of the local dielectric constant, and ρ_e is the free charge per unit volume. Gradations in the dielectric constant arise from the factors mentioned earlier. Free charge stems from the polarizing action of the applied field on ions that carry the current. To calculate the flow field arising from the action of these electrical body forces, the Stokes equations must be solved; clearly, one must know how the dielectric constant, charge and electric field are distributed to do this[8,17]. In our calculation, we take account of effects due to the polarization force and the force engendered by free charge created by the action of the imposed field in regions where the dielectric constant and conductivity vary smoothly. Accordingly, in addition to the Stokes equations, we employ equations for transport of charge along with the relation between charge and potential, and solve for the flow field numerically.

A qualitative picture of the flow patterns can be obtained from a simple model where the dielectric constant and conductivity distributions are prescribed. This was done for situations where a transverse electric field acts on a circular region with dielectric constant ε_1 and conductivity σ_1, surrounded by a region with properties σ_2 and ε_2; each property varies smoothly in the (thin) transition zone. Figure 3 depicts the situation and shows the streamlines of the velocity field calculated when the dielectric constant and conductivity of the interior exceed those in the exterior. In this case the dispersion would be drawn out into a ribbon-like shape oriented parallel to the field. (In three dimensions the shape would be ellipsoidal.) The flow direction reverses when the conductivity of the interior is less than that of the exterior, and the sample takes up a flat configuration orthogonal to the field. These features are in complete agreement with our experimental observations.

The relation between the direction and strength of the flow is complicated by the large number of parameters involved. Generally, however, if the difference between the dielectric constants of the two regions is not too large, flow will be in the direction of the applied field if the interior conductivity exceeds that of the exterior. The sense of the flow reverses when the conductivities are reversed. For apolar liquids with low conductivities, electrical forces due to free charge and dielectric-constant variations each play a role.

Although the experiments presented here used $BaTiO_3$/castor oil dispersions, the technique is not restricted to this system. Indeed, provided that there exists a sufficient mismatch in conductivity and/or dielectric constant, any colloidal dispersion nested within any ambient fluid may be manipulated in a similar manner. An example is the observation of dispersion bands during protein electrophoresis. In such experiments, a fluid bolus containing protein molecules is immersed inside a buffer solution and exposed to an electric field. As the protein molecules migrate through the gel, becoming separated on the basis of charge, bands appear to grow in an orthogonal direction to the applied field. The formation of such band structures is suspected of involving electrohydrodynamic processes similar to the ones described here[8,17]. □

Received 12 September 1994; accepted 14 February 1995.

1. Lachman, I. M., Bagley, R. D. & Lewis, R. M. *Ceram. Soc. Bull.* **60,** 202–205 (1981).
2. Tummala, R. R. *et al. IBM J. Res. Dev.* **36,** 889–904 (1992).
3. Newnham, R. & Ruschau, G. R. *J. Am. Ceram. Soc.* **74,** 463–480 (1991).
4. Gast, A. P. & Zukoski, C. F. *Adv. Colloid Interface Sci.* **30,** 153–202 (1989).
5. Halsey, T. C. *Science* **258,** 761–766 (1992).
6. Zukoski, C. F. *A. Rev. Mater. Sci.* **23,** 45–78 (1993).
7. Rosensweig, R. E. *Ferrohydrodynamics* (Cambridge Univ. Press, New York, 1985).
8. Rhodes, P. H., Snyder, R. S. & Roberts, G. O. *J. Colloid Interface Sci.* **129,** 78–90 (1989).
9. Randall, C. A., Miyazaki, S., More, K. L., Bhalla, A. S. & Newnham, R. E. *Mater. Lett.* **15,** 26–30 (1992).
10. Dogan, F., Liu, J., Sarikaya, M. & Aksay, I. A. in *Proc. A. Meeting EMSA* Vol. 50 (ed. Bailey, G. W.) 304–305 (San Francisco Press, San Francisco, 1992).
11. Kingery, W. D., Bowen, H. K. & Uhlmann, D. R. *Introduction to Ceramics* (Wiley, New York, 1976).
12. Scott, J. F. & Paz de Araujo, C. A. *Science* **246,** 1400–1405 (1989).
13. Glass, A. M. *Mater. Res. Soc. Bull.* **13,** 16–20 (1988).
14. Hirata, Y. & Kawabata, M. *Mater. Lett.* **16,** 175–180 (1993).
15. Landau, D. & Lifshitz, E. M. *Electrodynamics of Continuous Media* (Pergamon, New York, 1960).
16. Russel, W. B., Saville, D. A. & Schowalter, W. R. *Colloidal Dispersions* (Cambridge Univ. Press, 1989).
17. Saville, D. A. *Phys. Rev. Lett.* **71,** 2907–2910 (1993).

ACKNOWLEDGEMENTS. We thank F. Dogan for processing the barium titanate powder. Partial support for M.T. was provided by the Fulbright Commission. This work was supported by the US Air Force Office of Scientific Research, and the Microgravity Science and Applications Division of NASA.

Silica aerogel films prepared at ambient pressure by using surface derivatization to induce reversible drying shrinkage

Sai S. Prakash*, C. Jeffrey Brinker*†‡, Alan J. Hurd§ & Sudeep M. Rao*

* University of New Mexico/Sandia National Laboratories Advanced Materials Laboratory, 1001 University Boulevard SE, Albuquerque, New Mexico 87106, USA
† Ceramic Synthesis and Inorganic Chemistry Department 1846,
§ Ceramic Processing Science Department 1841,
Sandia National Laboratories, Albuquerque, New Mexico 87185, USA

HIGHLY porous inorganic films have potential applications as dielectric materials, reflective and anti-reflective coatings, flat-panel displays, sensors, catalyst supports and super-insulating architectural glazings[1–3]. Aerogels[4] are the most highly porous solids known, and can now be prepared from inorganic[5] and organic[6,7] precursors with volume-fraction porosities of up to 99.9% (ref. 8). Aerogels are normally prepared by supercritical extraction of the pore fluid from a wet gel[1], which prevents the network collapse that is otherwise induced by capillary forces. But supercritical processing is expensive, hazardous and incompatible with the processing requirements of many potential applications,

‡ To whom correspondence should be addressed.